Journal of Structural and Construction Engineering, 13(04), 2026, pp. 23-41

Journal of Structural and Construction Engineering

www.jsce.ir

Performance Evaluation of Steel Moment-Resisting Frames with Viscous Dampers Using the Direct Displacement-Based Design Method

Hesam Azizi[1], Saeed Maleki[2], Jamal Ahmadi[3*], Mahdi Eghbali[3]

1- PhD Graduate in Structural Engineering, Faculty of Engineering, University of Zanjan, Zanjan, Iran
2- Ms.c Graduate in Structural Engineering, Faculty of Engineering, University of Zanjan, Zanjan, Iran
3- Associate Professor, Faculty of Engineering, University of Zanjan, Zanjan, Iran

ABSTRACT

In recent years, the performance-based design method (PBD) has gained significant attention as an advanced approach for designing different structures with predictable seismic behavior. Among various PBD methodologies, direct displacement-based design (DDBD) has emerged as a particularly effective method due to its ability to reliably achieve target performance levels under seismic loading. This study tries to evaluate the seismic performance of steel moment-resisting frames (SMRFs) equipped with viscous dampers using the DDBD approach and compares the results with conventional design methods. Three SMRFs, 3-, 6-, and 9-story configurations, were designed using nonlinear static analysis (pushover analysis). Key seismic response parameters, including inter-story drift ratios (IDR) and base shear forces, were extracted and analyzed. The findings of the study demonstrate that the DDBD method effectively meets target performance objectives, ensuring controlled structural behavior under seismic excitation. Furthermore, compared to traditional force-based design (FBD) methods, DDBD provides a higher safety margin and improved structural efficiency. The study concludes that DDBD is a robust and reliable design approach for steel moment frames incorporating viscous dampers. Its application not only enhances seismic resilience but also optimizes structural performance, reducing potential damage during earthquakes. These advantages make DDBD a preferred method for modern seismic design, particularly in damped structural systems.

ARTICLE INFO

Receive Date: 13 July 2025
Revise Date: 15 November 2025
Accept Date: 07 December 2025

Keywords:
Force-based design method
Special steel moment frames
Seismic evaluation
Inter-story drift ratio
Base shear

doi: 10.22065/jsce.2025.533555.3772

*Corresponding author: Jamal Ahmadi
Email address: j_ahmadi@znu.ac.ir

1. Introduction

In conventional structural engineering practices, the design of structures has traditionally been predicated on the criterion of resistance. However, empirical evidence derived from extensive studies and observations of various seismic events and structural failures has demonstrated that structures designed using this conventional approach often exhibit suboptimal performance under dynamic forces, particularly those induced by earthquakes. Consequently, to address the inherent limitations and deficiencies of traditional seismic design methodologies, an advanced paradigm known as "performance-based design" has been introduced. This approach aims to ensure that structures are designed to meet specific performance objectives under a range of loading conditions, with a particular emphasis on seismic loads. The fundamental objective of this methodology is to achieve predefined performance levels, thereby enhancing the structural resilience and safety under earthquake-induced forces [1].

The Direct Displacement-Based Design (DDBD) methodology has established itself as one of the most prevalent and widely adopted approaches for establishing the correlation between displacement and structural damage. Initially introduced by Priestley in 1993 [2], the DDBD method has since garnered significant attention and has been extensively applied across a diverse range of composite structural systems. Notable applications include its implementation in steel frames incorporating buckling-restrained braces (BRBs) [3], coupled wall systems with steel coupling beams [4], steel shear walls integrated with self-centering energy dissipation braces [5], steel frames featuring intentionally eccentric braces [6], and steel frames augmented with viscoelastic dampers [7,8]. Furthermore, the DDBD approach has been successfully employed in the design of isolated structures equipped with fluid viscous dampers [9]. Over time, the DDBD methodology has undergone continuous refinement and enhancement, with advancements incorporating considerations such as the influence of higher-order modes [10], inelastic structural responses [11], and the development of tailored lateral displacement profiles specific to various structural typologies [12,13]. These developments have further solidified the method's robustness and applicability in modern structural engineering practice.

Fluid viscous dampers (FVDs) represent one of the most effective passive control systems, widely recognized for their ability to enhance the seismic performance of structures during seismic events. By augmenting structural damping and dissipating energy, FVDs effectively mitigate inter-story drift ratios (IDRs) and limit inelastic deformations [14]. Owing to their demonstrated efficacy in structural applications, coupled with their versatility in placement within structural systems and the availability of established design methodologies, FVDs have gained substantial traction in the building industry [15]. Consequently, a significant body of research has been dedicated to evaluating the seismic behavior of structures incorporating various types of dampers, as well as the design methodologies employed for such systems (e.g., [16,17]). The foundational framework for the analysis and design of structures equipped with damping systems was initially delineated in the technical report by Ramirez et al. [18]. This methodology has been further codified in Chapter 18 of ASCE/SEI 7 [19], which outlines the design requirements for both the structural system and the damping system. Notably, ASCE/SEI 7 specifies the acceptance criteria for IDRs under the maximum considered earthquake (MCE) scenario. Kitayama et al. [20] conducted a comprehensive investigation into the seismic performance of structures equipped with FVDs, designed in compliance with the aforementioned standard, thereby validating its applicability and effectiveness.

The Direct Displacement-Based Design methodology has been further advanced as a performance-based design framework for structures incorporating FVDs. The primary objective of this approach is to achieve predefined performance levels in an optimized manner, thereby mitigating excessive conservatism inherent in the design process. In this context, Lin et al. [21] employed the DDBD procedure to design three steel structures integrated with four distinct types of passive energy dissipation devices, namely fluid viscous, viscoelastic, friction, and metallic yielding dampers. Their methodology involved an iterative process to ensure that the structures met the specified performance criteria. Notably, a uniform distribution pattern for damping coefficients along the height of the buildings was adopted in their study. Kim and Choi [22] subsequently refined the DDBD procedure to assess the seismic performance of existing structures. Their findings demonstrated that the performance levels attained through DDBD were consistent with those derived from inter-story drift ratios (IDRs) obtained via time-history analyses. Furthermore, as highlighted in [23] and corroborated by earlier research [24], the DDBD methodology also advocated for a similar approach in designing structures equipped with supplemental damping systems. However, subsequent investigations, including those referenced in [7,25], have indicated that the DDBD approach, when applied to steel Moment-Resisting Frames (MRFs), tends to result in overdesigned structural configurations.

Bruschi et al. [26] introduced a straightforward and cost-effective design methodology for the seismic retrofitting of frame structures incorporating hysteretic dampers. The efficacy of this approach in attaining the desired displacement targets was substantiated through illustrative case studies. In a separate investigation, the performance-based seismic design framework and associated vulnerability assessments were meticulously examined and evaluated [27]. The analytical findings demonstrated that the performance-based design methodology is well-suited for the design of concrete frames integrated with metallic dampers, with the latter significantly enhancing the seismic resilience of conventional concrete frames. Li et al. [28] advanced a substructure-based design (SBD) approach, specifically tailored for vertically irregular steel buckling-restrained braced frame structures (VSBFSs). This method involves isolating the substructures of each story within a VSBFS from the

global structural system, enabling individual analysis in subsequent design phases. Mustafa et al. [29] delineated the DDBD for coupled shear wall (CSW) systems incorporating two distinct types of energy dissipation dampers within the coupling beams: metallic dampers and viscoelastic dampers.

In light of the critical role of structural control in mitigating seismic-induced damage, this study delves into the efficacy of viscous fluid dampers by executing a rigorous comparative analysis. The structural design incorporating these dampers is performed using both force-based (FBD) and direct displacement-based (DDBD) approaches, a framework that facilitates a direct evaluation of their respective contributions to achieving desired performance benchmarks. While the principles of DDBD are established, this study provides a novel, comprehensive evaluation of its efficacy for steel moment-resisting frames equipped with nonlinear viscous dampers. The primary innovations are threefold: first, it conducts a direct and systematic performance comparison between DDBD and the conventional FBD method for a dual lateral system where base shear is strategically shared. Second, it critically investigates the impact of damper distribution, contrasting the optimized non-uniform pattern from DDBD with the uniform assumption typical in FBD, on the seismic response of low- to mid-rise structures. Finally, the study tries to provide evidence-based insights into inelastic behavior, including plastic hinge distribution, and delivers practical recommendations for refining design methodologies. Through this approach, the research aims to deliver a validated framework for achieving enhanced seismic performance and resilience in damped steel frame structures.

2-Direct Design Methods

2.1. Direct Displacement based design (DDBD) method

The direct displacement-based design methodology is predicated on the substitution of a nonlinear multi-degree-of-freedom (MDOF) structure with an equivalent linear single-degree-of-freedom (SDOF) system, as illustrated in Fig. 1a [25]. To achieve this, a design deformation mode is postulated for the MDOF structure, and the dynamic properties of the corresponding SDOF system, including effective height, effective mass, and target displacement, are derived based on this assumed deformation mode. The force-displacement relationship for the nonlinear SDOF system is depicted in Fig.e 1. Given that the linear displacement spectrum is directly utilized in the displacement-based design process, the nonlinear SDOF system is rendered equivalent to a linear SDOF system characterized by a constant stiffness, as demonstrated in Fig. 1b. This equivalence is established by representing the energy dissipated through the hysteretic behavior of the nonlinear system as an equivalent viscous damping, which is functionally dependent on the system's required ductility. Fig. 1c illustrates the equivalent viscous damping for a steel moment frame system, determined as a function of structural ductility. The effective period of the SDOF system is subsequently calculated using the linear displacement spectrum, corresponding to the desired equivalent damping at the target displacement, as shown in Fig. 3d. Ultimately, the design base shear is computed based on this effective period and the target displacement.

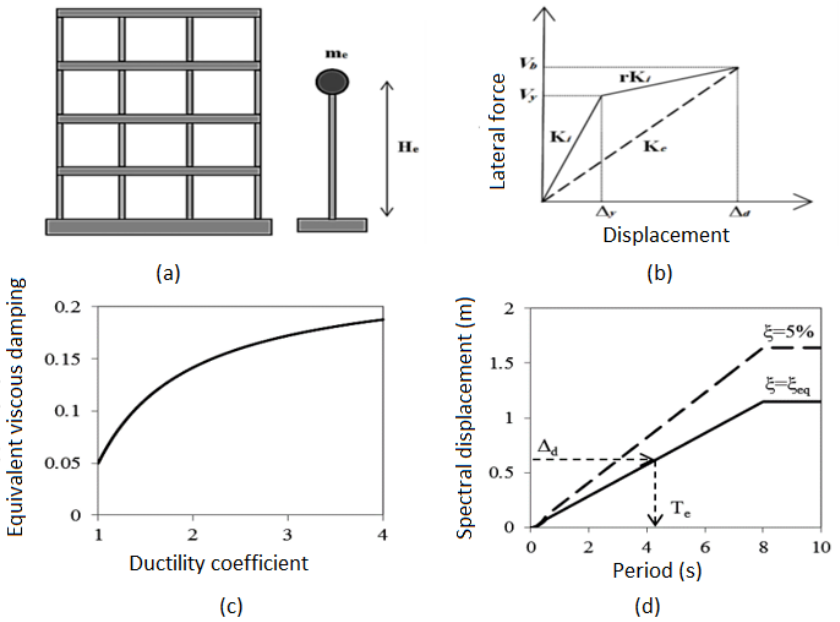

Figure 1. Fundamental methodology of the DDBD approach: (a) Equivalent SDOF system; (b) Nonlinear behavior of the equivalent SDOF system; (c) Equivalent viscous damping; (d) Displacement response spectrum [25].

The design methodology employing direct displacement-based principles for structures incorporating nonlinear viscous dampers can be systematically delineated as follows:

Step 1) The target displacement corresponding to the critical class, aligned with the desired performance level, is to be determined.

Step 2) The displacements of the remaining classes are subsequently derived based on the critical class and the deformation mode, utilizing Eq. 1 as referenced in [23].

$$\Delta_i = \omega_\theta \theta_c h_i \left(\frac{4H_n - H_i}{4H_n - h_i} \right) \tag{1}$$

In this context, H_i is defined as the height of the ith floor measured from the base, while H_n represents the total height of the structure. The height of the first floor of the structure is denoted as H_1. The target displacement value is expressed as θ_c, and ω_θ is a coefficient introduced to account for the influence of higher modes. This coefficient is derived through the application of Eq. 2.

$$\omega_\theta = 1.15 - 0.0034 H_n \leq 1.0 \tag{2}$$

Step 3) The target displacement of the alternative one-degree-of-freedom structure is determined through the application of Eq. 3 [23].

$$\Delta_d = \frac{\sum_{i=1}^{n} \left(m_i \Delta_i^2 \right)}{\sum_{i=1}^{n} \left(m_i \Delta_i \right)} \tag{3}$$

In this context, the mass of the ith floor is denoted as mi, while the displacement of the ith floor is represented by Δ_i.

Step 4) The mass and effective height of the single-degree-of-freedom structure, as opposed to the multi-degree-of-freedom structure, are determined utilizing relations (4) and (5) [23].

$$m_e = \frac{\sum_{i=1}^{n} \left(m_i \Delta_i \right)}{\Delta_d} \tag{4}$$

$$H_e = \frac{\sum_{i=1}^{n} \left(m_i \Delta_i H_i \right)}{\sum_{i=1}^{n} \left(m_i \Delta_i \right)} \tag{5}$$

In these relations, me and H_e represent the effective mass and effective height, respectively.

Step 5 involves the determination of the plasticity coefficient value in the target displacement through the application of relation (6) [30,31].

$$\mu = \frac{\Delta_d}{\Delta_y} \tag{6}$$

The value of Δ_y, representing the yield displacement of the structure, is determined through the application of Eq. 7 as referenced in [1].

$$\Delta_y = \theta_y H_e \tag{7}$$

In this context, θ_y represents the yield angle, the value of which is derived for steel structural frames through the application of relation (8) [1].

$$\theta_y = 0.65 \varepsilon_y \frac{L_b}{h_b} \tag{8}$$

In these relationships, L_b represents the span length of the beam measured between the centers of the columns, h_b denotes the depth of the beam, and ε_y corresponds to the yield strain of the steel.

Step 6) The equivalent viscous damping is determined, encompassing the linear damping of the structure, the hysteresis damping, and the equivalent damping contributed by the viscous damper, as defined by Eq. 9 [23].

$$\xi_{eq} = \xi_{el} + \xi_{hyst} + \xi_{VD} \tag{9}$$

In this context, ξ_{el} represents the linear damping coefficient of the structure, which is conventionally assumed to be 5% for steel frames. Meanwhile, ξ_{hyst} denotes the hysteresis damping, which is derived for the steel bending frame through the application of Eq. 10 [16], utilizing the ductility coefficient as a key parameter.

$$\xi_{eq} = 0.05 + 0.577\left(\frac{\mu - 1}{\mu\pi}\right) \tag{10}$$

Step 7) The damping coefficient ξ_{VD}, attributable to the nonlinear fluid viscous damper, is determined utilizing Eq. 11 as referenced in [23].

$$\xi_{VD} = \frac{1}{4\pi}\frac{E_{VD}}{E_s} = \frac{1}{4\pi} \times \frac{\pi C_d \omega^{\alpha} u_0^{\alpha+1} \lambda}{k u_0^2 / 2} = \frac{C_d \omega^{\alpha} u_0^{\alpha} \lambda}{2 k u_0} = \frac{\lambda F_d}{2V} = \frac{\lambda \beta}{2} \tag{11}$$

Step 8) Determination of the effective time period

The effective period of a SDOF system is derived through the utilization of the displacement spectrum. Initially, the displacement design spectrum corresponding to the specified equivalent damping percentage must be established. It should be noted that the standard design spectra are typically provided for a damping percentage of 5%. Consequently, this baseline design spectrum is required to be scaled by the coefficient specified in Eq. 12 to obtain the displacement design spectrum for the target damping percentage [21].

$$R_{\xi} = \left(\frac{0.1}{0.05 + \xi_{eq}}\right)^{0.5} \tag{12}$$

The effective period is subsequently calculated based on the derived displacement spectrum and the specified target design displacement, as illustrated in Fig. 1d.

Step 9) Determination of Design Base Shear Force

The design base shear force is calculated in accordance with the effective period and the target design displacement, as defined by Eq. 13:

$$V_b = K_e \Delta_d \;\&\; K_e = \frac{4\pi^2 m_e}{T_e^2} \tag{13}$$

In these equations, Te and ke represent the natural period and effective stiffness of an equivalent single-degree-of-freedom (SDOF) system, respectively.

Step 10) Design-Based Shear Force Distribution

The distribution of design shear forces is derived based on the predefined displacement profile, as formulated in Eqs. 14 and 15 [23].

$$F_i = k V_b \frac{m_i \Delta_i}{\sum_{i=1}^{n} m_i \Delta_i} \qquad \text{For 1 to n-1 stories} \tag{14}$$

$$F_i = (1-k) V_b + k V_b \frac{m_i \Delta_i}{\sum_{i=1}^{n} m_i \Delta_i} \qquad \text{For n-story} \tag{15}$$

In this context, the value of K is established as 0.9 for frames comprising 10 or more stories, while a value of 1 is assigned to frames with fewer stories.

Step 11) Determination of the damping coefficient for the nonlinear viscous fluid damper.

The damping coefficient of the nonlinear viscous fluid damper at each story of the structure is computed utilizing Eq. 16 [25].

$$C_i = \frac{F_{d,i}}{(\eta_i S_V)^{\alpha}} = \frac{F_{d,i}}{(\eta_i \omega S_d / \Upsilon)^{\alpha}} = \frac{F_{d,i}\,(\Upsilon T_e)^{\alpha}}{(2\pi\eta_i \Delta_{d,i})^{\alpha}} \tag{16}$$

In this context, S_v and S_d are defined as the spectral velocity and spectral displacement, respectively, while α, γ, and η represent the coefficients associated with the viscous damper.

2.2. Force-Based Design Method

In this investigation, the force-based design methodology is implemented in accordance with the 2800 standard, fourth edition [32]. Initially, a parameter referred to as the earthquake coefficient is computed, and through its multiplication by the effective seismic weight, the base shear of the structure is derived. Subsequently, the resultant shear force is analyzed and systematically distributed across the floors of the structure, with the design process being conducted under the influence of these forces. Following the design of the structural sections, it is imperative that the maximum drift values of the floors do not exceed the permissible limits as stipulated. Furthermore, Eq. 17 has been utilized to determine the damping associated with viscous dampers within this framework.

$$\xi_i = \frac{\lambda \sum_{j=1}^{n} C_j \phi_{rj}^{1+\alpha} \cos^{1+\alpha}(\theta_j)}{A_i^{1-\alpha} \omega_i^{2-\alpha} \sum_{j=1}^{n} m_i \varphi_j^2} \quad (17)$$

In this context, λ is defined as a constant coefficient, while ϕ_{rj} represents the absolute modal displacement corresponding to each story. The maximum displacement of the structure under seismic excitation, associated with the spectral acceleration related to the damping of the entire structure, is denoted by A_i. The damper angle at each story is expressed as θ_j, and ω_i is identified as the angular frequency of the ith mode of the structure, typically corresponding to the first mode. Additionally, m_j is designated as the mass of the respective story.

3- Modeling

3.1. Geometry, Loading, and Modeling

To facilitate the analytical investigations, the structural frame models presented in this study were developed using the finite element software SAP2000. Initially, the frame models were constructed and designed in two configurations: one without dampers and the other incorporating dampers. These models were subsequently subjected to equivalent static analysis, performed linearly within the software. The study aimed to evaluate the performance of optimal bending steel frames equipped with viscous dampers, utilizing a direct design methodology grounded in both displacement-based and force-based principles. For this purpose, two-dimensional frames with special ductility, comprising 3, 6, and 9 stories, were modeled and analyzed. These frames were specifically selected to assess the efficacy of the proposed design approach under varying structural heights.

The frames under investigation comprise five spans, each measuring six meters in length. The height remains consistent across all floors, standardized at 3.3 meters. The gravity loads imposed on the structures are designed in compliance with the sixth section of the National Building Regulations, 2013 edition [33], while the lateral seismic forces are derived from the fourth edition of Standard 2800 [32]. The preliminary design of the structural member cross-sections is conducted in accordance with the tenth section of the National Building Regulations, 2013 edition [34]. The steel selected for the frame members is of type ST37, characterized by a yield strength of 240 MPa. Seismic loading for the structures has been estimated under the assumption that they are situated on type 2 soil, as specified in Standard 2800 [32]. The effective mass of the structure during seismic events is determined by considering dead loads in addition to a 20% contribution from live loads. The values of the applied gravity loads are detailed in Table 1. Following the determination of the cross-sections from the initial structural design, a nonlinear model of the structures was developed by defining plastic hinges within the first 5% of the beam and column elements, based on [35], to facilitate nonlinear time history analysis. Furthermore, the Link element was utilized in a nonlinear manner to model the viscous damper within the SAP2000 software.

Table 1. Design Values of Gravitational Loads.

Type of load according to(kPa)	**Load quantity**
Dead (ceiling of floors)	6
Dead (ceiling of the roof)	6.5
Dead (perimeter wall)	7.5
Dead (Roof shelter)	2.5
Live (Floor)	2
Live (Roof)	1.5

3.2. Damper Characteristics

In the present study, the behavior of the dampers is characterized as nonlinear, with the Maxwell model being employed for analysis. Within this framework, stiffness and damping are modeled in series, aligned in parallel with one another. For the viscous damper representation, a sufficiently large and physically justified value is assigned to the stiffness parameter. The damping parameter is defined as equivalent to the damping coefficient derived from both the force and displacement methodologies. Additionally, the coefficient α is assigned a value of 0.5, while the coefficients η and γ are both set to unity.

3.3. Sectional Specifications

As previously indicated, within the scope of this investigation, special steel moment frames comprising 3, 6, and 9 stories were designed utilizing the SAP2000 software. Two direct design methodologies, displacement-based and force-based, were employed under equivalent static analysis, considering scenarios both with and without the incorporation of viscous dampers. The resulting beam and column sections for the 3-, 6-, and 9-story frames are systematically detailed in Tables 2, 3, and 4, respectively. From the derived sectional data, it is evident that the application of the displacement-based method results

in an enlargement of the structural cross-sectional dimensions across all cases. Conversely, the integration of viscous dampers within both design methodologies has been observed to yield a substantial reduction in sectional dimensions, thereby contributing to a notable decrease in the overall structural weight.

Table 2. Designed Sections of the Three-Story Structural Framework.

		Force method			Displacement Method		
Structural mode	**Story**	**Internal column sections**	**Side column sections**	**Beam sections**	**Internal column sections**	**Side column sections**	**Beam sections**
Without damper	1	W12×79	W12×58	W10×39	W12×120	W12×87	W10×68
	2	W12×79	W12×58	W10×39	W12×120	W12×87	W10×60
	3	W12×58	W12×35	W10×30	W12×87	W12×58	W10×39
With damper	1	W12×79	W12×58	W10×39	W12×106	W12×87	W10×60
	2	W12×79	W12×58	W10×39	W12×106	W12×87	W10×54
	3	W12×53	W12×35	W10×26	W12×79	W12×58	W10×39

Table 3. Designed Sections of the Six-Story Structural Framework.

		Force method			Displacement method			
Structural mode	**Story**	**Internal column sections**	**Side column sections**	**Beam sections**		**Internal column sections**	**Side column sections**	**Beam sections**
Without damper	1	W14×109	W14×53	W14×38	W14×61	W14×38	W14×145	W14×82
	2	W14×109	W14×53	W14×38	W14×61	W14×38	W14×145	W14×82
	3	W14×109	W14×48	W14×38	W14×53	W14×38	W14×120	W14×68
	4	W14×82	W14×48	W14×34	W14×48	W14×34	W14×109	W14×68
	5	W14×82	W14×38	W14×30	W14×38	W14×30	W14×109	W14×53
	6	W14×61	W14×38	W14×26	W14×26	W14×26	W14×82	W14×53
With damper	1	W14×82	W14×53	W14×30	W14×38	W14×30	W14×109	W14×68
	2	W14×82	W14×53	W14×30	W14×38	W14×30	W14×109	W14×53
	3	W14×74	W14×38	W14×30	W14×38	W14×30	W14×109	W14×53
	4	W14×68	W14×38	W14×26	W14×38	W14×26	W14×82	W14×53
	5	W14×53	W14×34	W14×26	W14×26	W14×26	W14×82	W14×48
	6	W14×53	W14×34	W14×26	W14×26	W14×26	W14×68	W14×48

Table 4. Designed Sections of the Nine-Story Structural Framework.

		Force method				Displacement-based method		
Structural mode	**Story**	**Internal column sections**	**Side column sections**	**Beam sections**		**Internal column sections**	**Side column sections**	**Beam sections**
Without damper	1	W18×119	W16×77	W16×40	W16×50	W16×40	W18×130	W16×89
	2	W18×119	W16×77	W16×40	W16×50	W16×40	W18×130	W16×77
	3	W18×106	W16×77	W16×40	W16×50	W16×40	W18×130	W16×77
	4	W18×106	W16×57	W16×40	W16×50	W16×40	W18×119	W16×77
	5	W18×86	W16×57	W16×36	W16×50	W16×36	W18×119	W16×77
	6	W18×86	W16×57	W16×36	W16×40	W16×36	W18×106	W16×77
	7	W18×76	W16×40	W16×31	W16×40	W16×31	W18×97	W16×77
	8	W18×65	W16×40	W16×31	W16×31	W16×31	W18×65	W16×40
	9	W18×65	W16×40	W16×26	W16×26	W16×26	W18×65	W16×40
With damper	1	W18×106	W16×57	W16×31	W16×40	W16×31	W18×119	W16×67
	2	W18×106	W16×57	W16×31	W16×40	W16×31	W18×119	W16×67
	3	W18×86	W16×57	W16×31	W16×40	W16×31	W18×106	W16×67
	4	W18×86	W16×45	W16×31	W16×36	W16×31	W18×97	W16×57
	5	W18×76	W16×45	W16×31	W16×36	W16×31	W18×97	W16×57
	6	W18×76	W16×45	W16×31	W16×31	W16×31	W18×86	W16×40
	7	W18×76	W16×36	W16×31	W16×31	W16×31	W18×87	W16×40
	8	W18×60	W16×36	W16×31	W16×31	W16×31	W18×65	W16×40
	9	W18×60	W16×36	W16×26	W16×26	W16×26	W18×65	W16×40

The damping coefficients associated with the viscous damper, as determined by the two design methodologies for 3-, 6-, and 9-story structures, are presented in Tables 5 through 7, respectively. It is noteworthy that within the force-based design approach, the damping coefficient of the damper is uniformly assumed across all stories, and the design process is predicated on this assumption.

Table 5. Damping coefficients of viscous dampers in a three-story structure.

Design method	**Story**	**Damping** (KN.s/m) **coefficient**
Force-based method	All Stories	90.49
Displacement-based method	1	236.64
	2	190.15
	3	97.18

Table 6. Damping coefficients of viscous dampers in a Six-story structure.

Design method	story	Damping (KN.s/m) coefficient
Force-based	All stories	171.95
displacement-based	1	433.53
	2	411.19
	3	366.51
	4	299.48
	5	249.33
	6	98.39

Table 7. Damping coefficients of viscous dampers in a Nine-story structure.

Design method	story	Damping (KN.s/m) coefficient
Force-based	All stories	239.91
displacement-based	1	544.18
	2	531.41
	3	505.87
	4	467.55
	5	416.46
	6	352.6
	7	275.96
	8	186.55
	9	84.37

4- Validation

The numerical modeling approach employed in this study was subjected to a multi-level validation process. While direct comparison with a full-scale experimental test was not feasible due to the scarcity of publicly available data for the specific structural system under investigation, the following steps were taken to ensure the reliability and accuracy of the numerical models.

4.1. Validation of Moment Frames

The modeling of steel moment resisting frames in SAP2000 software was validated by recreating a benchmark 9-story steel frame model from the SAC Phase II Steel Project [36, 37]. The SAC project was a joint venture of the Structural Engineers Association of California (SEAOC), the Applied Technology Council (ATC), and California Universities for Research in Earthquake Engineering (CUREE), established to address the performance of steel moment frames following the 1994 Northridge earthquake. The benchmark structures, designed by the engineering firm Brandow & Johnston Associates, are code-compliant designs representing typical construction for the Los Angeles, California region. Although not physically constructed, these models have been extensively validated and serve as internationally recognized benchmarks, providing a robust basis for comparing analytical results across the research community.

The structural model, along with the cross-sectional properties of the beams and columns, is illustrated in Fig. 2. The basement and ground floor heights were specified as 3.65 meters and 5.49 meters, respectively, while the remaining floors were modeled with a uniform height of 3.96 meters. The span length was set at 9.15 meters, and the yield strengths of the steel utilized in the beams and columns were defined as 245 MPa and 348 MPa, respectively.

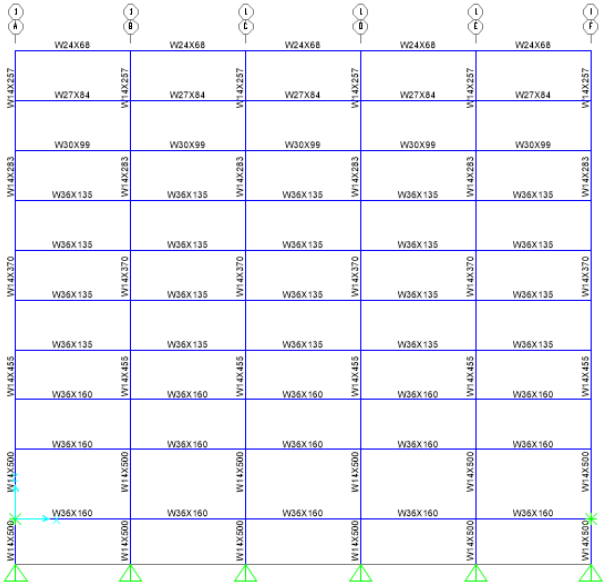

Figure 2. Structural modeling of the nine-story SAC [36] in the SAP2000 software.

The periodicity times corresponding to the first three modes of the structure are presented in Table 8. As evidenced by the data, the results obtained demonstrate a strong concordance with those reported in the referenced SAC studies [36], thereby validating the accuracy of the studied structural modeling approach.

Table 8. Comparison of the natural periods of the modeled frame in SAP2000 with the reference model.

First mode period (s)		Second mode period (s)		Third mode period (s)	
Study[36]	Model SAP	Study[36]	Model SAP	Study[36]	Model SAP
2.27	2.27	0.85	0.85	0.49	0.49

4.2. Verification of Viscous Dampers

To validate the modeling of viscous dampers within the SAP2000 software, a single-story, single-span frame with a height of 3 meters and a span length of 6 meters was constructed in both SAP2000 and ETABS software, as illustrated in Fig. 3. The roof displacement over time was analyzed under the excitation of the Tabas earthquake recorded at Ferdows Station (identified by ID number 140 on the PEER website), which exhibited a peak ground acceleration of 0.105 g. The damping coefficient and the exponent α for the viscous damper were specified as 12 kN·s/mm and 1, respectively. The beam and column cross-sections were designated as W12x40 and Box20x20x2, respectively. Furthermore, the bracing elements were modeled with a circular cross-section of 1 meter in diameter to ensure rigid behavior. The material properties of the steel were defined as St37.

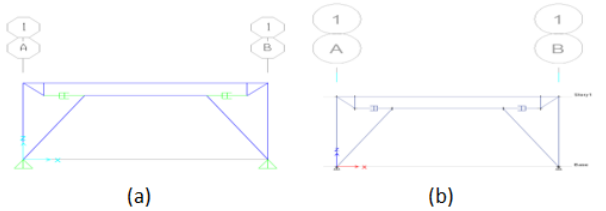

Figure 3. illustrates the modeling of a single-story, single-bay frame in (a) SAP2000 and (b) ETABS.

The displacement of the structure under time history analysis during the seismic event was determined, as illustrated in Fig. 4. Upon comparison of the two graphs, it is evident that the responses derived from the respective software programs exhibit a high degree of concordance.

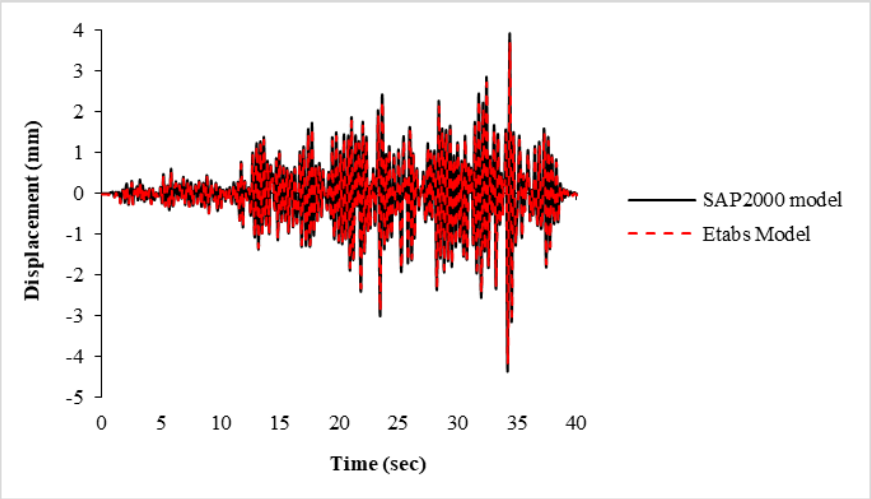

Figure 4. Comparative analysis of the frame displacement of a single-span, single-story structure during the seismic event.

5- Accelerograms

Accelerograms utilized for dynamic analyses are required to exhibit characteristics that closely align with those of a probable seismic event at the construction site, thereby ensuring compliance with the design earthquake criteria. To achieve this, it is imperative that the selected accelerograms possess attributes, such as magnitude, fault distance, and seismic source mechanism, that are optimally representative of the structural site conditions. Furthermore, the geological, tectonic, and seismic characteristics of the site from which each accelerogram is derived should exhibit a high degree of similarity to those of the construction site, with particular emphasis on the properties of the soil strata.

In this investigation, seven accelerograms were employed for the seismic analysis of models using nonlinear time history analysis according [38,39]. These accelerograms, the detailed characteristics of which are tabulated in Table 9, were sourced from the PEER database. The pseudo-acceleration spectrum for each accelerogram, along with their mean spectrum, is illustrated in Fig. 6. The selected accelerograms were scaled in accordance with the spectrum specified by the standard design code 2800 [32], following the methodology outlined therein. The derived scaling factors are documented in Table 10.

6- Nonlinear Dynamic Analysis

To fulfill the primary objective of this study, which is to provide a direct, quantitative performance comparison between Force-Based and Direct Displacement-Based Design methodologies for steel moment-resisting frames with nonlinear viscous dampers, the investigated frames were subjected to nonlinear dynamic analysis. This approach was essential to evaluate the influence of each design methodology and the incorporation of dampers on the structure's seismic performance beyond elastic limits. The analysis utilized seven specified accelerograms and was conducted using SAP2000 software. The structures were initially loaded with a gravity combination of 1.1DEAD+0.275LIVE. The dynamic solution was carried out via direct integration using the Newmark method, with beta and gamma coefficients set to 0.25 and 0.5, respectively, to generate the practical insights into inelastic hinge development and damper efficiency that form the core contribution of this work.

Table 9. Characteristics of the Selected Earthquakes.

Earthquake ID in the study	Event name	Station name	Earthquake number in the database PEER	magnitude	D5-95 (s)
EQ1	Kocaeli	Eregli	1159	7.51	18.7
EQ2	Kocaeli	Iznik	1166	7.51	19.5
EQ3	Kocaeli	Mecidiyekoy	1170	7.51	16.5
EQ4	Kocaeli	Tekirdag	1172	7.51	12.1
EQ5	Duzce	Lamont	1616	7.14	20.5
EQ6	Duzce	Mudurnu	1619	7.14	16.4
EQ7	Caldiran	Maku	1627	7.14	20.7

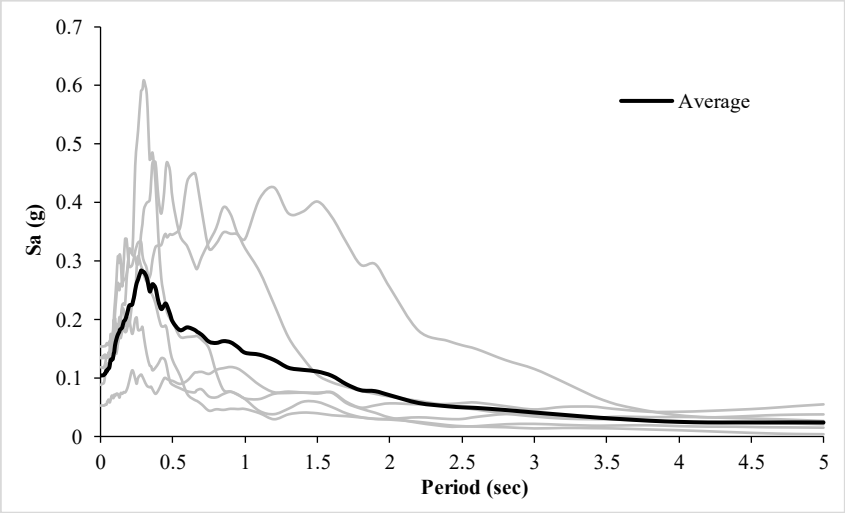

Figure 5. The pseudo-acceleration spectra of the selected seismic events, accompanied by their mean values.

Table 10. Scaling coefficients of accelerograms.

Structure	Without damper	With damper
3story	0.571	0.3926
6story	0.4622	0.3175
9story	0.3544	0.2664

7- Discussion

This section presents a discussion of the results derived from the nonlinear time history analyses, offering a detailed comparison of the seismic performance of frames designed using the FBD and DDBD methodologies. The evaluation begins with an assessment of key engineering demand parameters, including inter-story drift and base shear, to establish a baseline for comparison. Subsequently, the discussion delves into nuanced aspects of structural behavior, exploring the critical influence of damper coefficient distribution, the robustness of the findings against variations in soil type and material properties, and the resultant inelastic hinge mechanisms.

7.1. Relative Lateral Displacement of Structures

For the purpose of comparative analysis, the average story drift (relative lateral displacement) of the structures subjected to seven accelerograms has been extracted. The mean values of story drift for the 3-, 6-, and 9-story frames are illustrated in Fig. 6. Furthermore, the maximum value derived from the average story drift values is tabulated in Table 11. It is evident that the incorporation of a nonlinear viscous damper within the force-based and displacement-based design methodologies for the 3-story structure has resulted in a reduction of the maximum average drift value by 60% and 55.6%, respectively. Additionally, the application of the displacement-based design method in structures devoid of dampers has yielded a 3.6% reduction in structural drift. In the case of the 6-story structure, the implementation of a damper within the force-based and displacement-based design approaches has led to a decrease in the maximum average drift value by 58.88% and 68.92%, respectively. Conversely, the utilization of the displacement-based design method in structures without dampers has been associated with a 10.8% increase in structural drift. For the 9-story structure, the integration of a nonlinear viscous damper in the force-based and displacement-based design methods has resulted in an increase of 27% and a reduction of 15%, respectively, in the maximum average drift. Moreover, the application of the displacement-based design method in structures without dampers has facilitated a 10.4% reduction in structural drift.

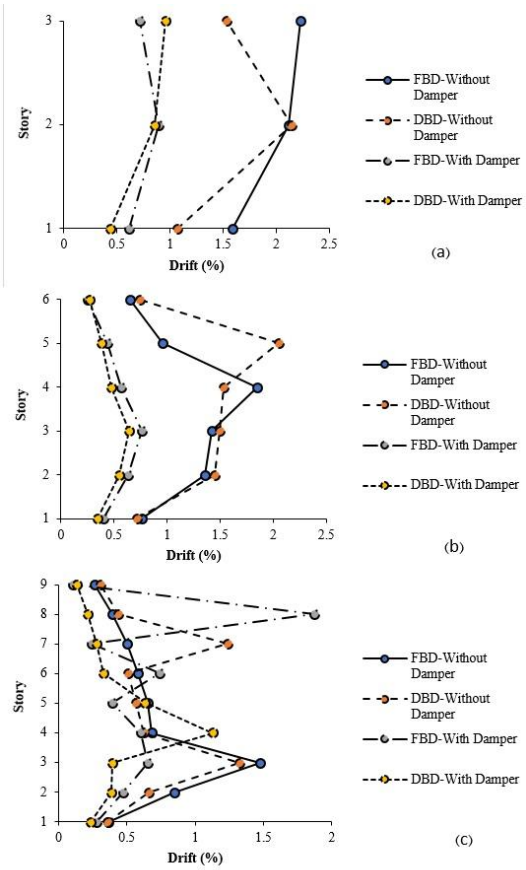

Figure 6. Average drift levels across various structural configurations: (a) three-story, (b) six-story, and (c) nine-story buildings.

Table 11. The maximum value derived from the mean drift values across various classes.

Structure drift (%)				
Structure	**Force-based method**		**displacement-based method**	
	Without damper	**With damper**	**Without damper**	**With damper**
3story	2.23	0.89	2.15	0.95
6story	1.85	0.76	2.05	0.64
9story	1.47	1.87	1.32	1.13

7.2. Base Shear

In this section, a comparative analysis of the base shear derived from nonlinear time history analyses is presented for structures evaluated under two distinct design methodologies, force-based and displacement-based, both with and without the incorporation of dampers. The results pertaining to the average base shear for the investigated structures are illustrated in Fig. 7. The average base shear is computed as the mean value derived from the application of seven accelerograms to the structures. As evidenced by the figure, the implementation of a nonlinear viscous damper in the 3-story structure has resulted in a substantial reduction in the average base shear, with reductions quantified at 48.19% for the force-based design method and 56.86% for the displacement-based design method. As anticipated, owing to the increased dimensions of structural members designed using the displacement-based approach, the base shear values for both scenarios, with and without dampers, were observed to be 14% and 37% higher, respectively, compared to those designed using the force-based method.

For the 6-story structure, the incorporation of a nonlinear viscous damper led to a reduction in the average base shear by 48.82% in the force-based design method and by 58.41% in the displacement-based design method. Furthermore, the base

shear values for the displacement-based design method, both without and with dampers, were found to be 44.4% and 17% higher, respectively, than those obtained using the force-based design method. In the case of the 9-story structure, the average base shear was reduced by 30.76% in the force-based design method and by 30.73% in the displacement-based design method due to the inclusion of a viscous damper. For the displacement-based design method, the base shear values, both without and with dampers, were 16.41% and 16.5% higher, respectively, compared to those derived from the force-based design method. These findings underscore the influence of design methodology and damping systems on the structural response, particularly in terms of base shear reduction.

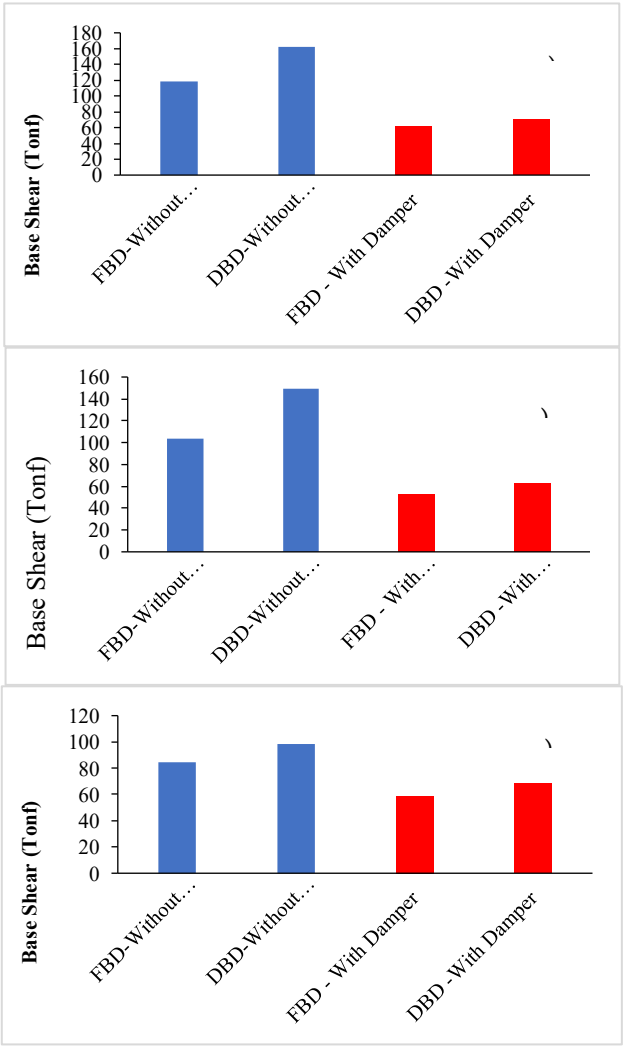

Figure 7. Mean base shear in the structure for (a) 3-story, (b) 6-story, and (c) 9-story configurations.

7.3 Effect of Damper Coefficient Distribution

The distribution pattern of the viscous damper coefficients significantly influences the seismic performance of the frames. As detailed in Tables 5 to 7, the FBD method employed a uniform distribution (UD) of coefficients, whereas the DDBD method yielded a non-uniform distribution (NUD) that decreases with height, aligning more closely with the typical profile of inter-story shear forces.

The results for maximum inter-story drift (Table 11) indicate that the NUD generally provides more effective control, particularly for the 6- and 9-story frames. For the 6-story frame, the NUD reduced the maximum drift by 15.8% compared to the UD (0.64% vs. 0.76%). This superiority is even more pronounced in the 9-story frame, where the NUD achieved a 39.6% lower drift than the UD (1.13% vs. 1.87%). This can be attributed to the fact that the UD approach provides excess damping capacity in the upper floors, where seismic demands are lower, while potentially providing insufficient damping in the lower

floors, where demands are highest. The NUD, by concentrating damping resources where they are most needed, leads to a more efficient and optimized structural response. For the 3-story frame, the difference was less significant, suggesting that the benefits of an optimized distribution become more critical as the frame height and the influence of higher modes increase. A direct comparison of the maximum drift for frames with dampers, presented in Table 12, clearly demonstrates the superior effectiveness of the non-uniform distribution from the DDBD method in mid- and high-rise structures.

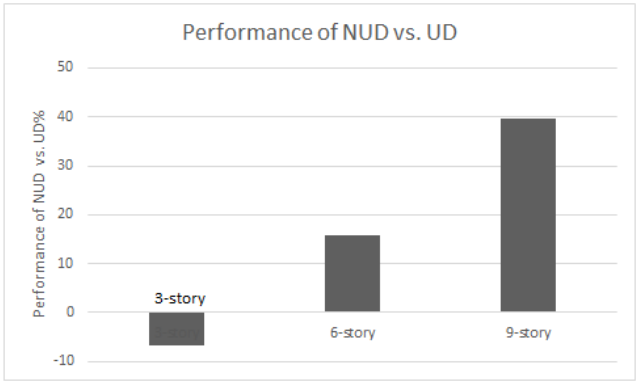

Figure 8. Comparison of Maximum Inter-Story Drift (%) for Uniform (FBD) vs. Non-Uniform (DDBD) Damper Distributions.

7.4 Influence of Soil Type and Design Spectrum

Acknowledging the importance of site-specific seismic hazards, a supplementary sensitivity analysis was conducted to investigate the effect of soil type on the comparative performance of the FBD and DDBD methods. The 6-story frame was redesigned for Soil Type I (stiff soil) and Soil Type IV (soft soil), as defined by Iranian Code 2800, in addition to the original Soil Type II (medium soil). The structures were then analyzed under the same suite of seven accelerograms, scaled appropriately for each soil type's design spectrum.

The results, summarized in Table 12, confirm that the absolute seismic demands are highly sensitive to the site condition. As expected, softer soils (Type IV) lead to significantly higher inter-story drifts and base shears due to greater spectral amplifications, while the opposite is true for stiffer soils (Type I).

Table 12. The effect of soil type on the maximum inter-story drift for each design method.

Soil Type	FBD - Max Drift (%)	DDBD - Max Drift (%)
I (Stiff)	0.60	0.48
II (Medium)	0.76	0.64
IV (Soft)	1.10	0.85

Crucially, however, the comparative performance between the two design methodologies remains consistent across all soil types. As clearly indicated in Table 12, the maximum inter-story drift in the DDBD-designed frame is consistently lower than that of the FBD-designed frame for every soil class. This demonstrates that the fundamental advantage of the displacement-based design approach, superior and more predictable deformation control, is robust and not an artifact of a specific site condition. The efficiency gained by incorporating viscous dampers was also observed to be effective universally. This finding indicates that DDBD provides a more reliable framework for seismic design of damped steel frames than traditional FBD, independent of the local site class.

7.5 Discussion on Nonlinear Hinge Behavior

A detailed analysis of the nonlinear hinge formation was conducted to compare the inelastic performance of frames designed using the FBD and DDBD methods. The results, derived from the nonlinear time history analyses, reveal a fundamental difference in the damage distribution. In frames designed using the FBD method, the formation of plastic hinges was often less uniform, showing a tendency for inelasticity to concentrate in specific stories, particularly in the lower and middle floors. This can lead to the development of a soft-story mechanism under severe seismic loading, which is an undesirable failure mode.

Conversely, in frames designed using the DDBD method, a more uniform distribution of plastic hinges was observed along the height of the structure. This "global" mechanism is a direct outcome of the displacement-based design philosophy, which aims to achieve a predetermined deformation shape. By ensuring a more even distribution of yield capacity, the DDBD approach promotes a more stable and ductile structural response, where energy dissipation is spread throughout the frame rather than being localized. This results in lower average plastic hinge rotations in DDBD frames compared to FBD frames, confirming that DDBD not only controls elastic deformations but also provides a more robust and predictable inelastic performance by mitigating the risk of progressive collapse.

7.6 Parametric Sensitivity Analysis

A sensitivity analysis was conducted to evaluate the influence of key design parameters on the seismic performance. The 6-story frame was re-analyzed under two variations: a reduced viscous damper contribution (15% of base shear) and the use of a higher-strength steel (Grade 350 MPa). The results, presented in Table 13, indicate that while these parameter changes affect the absolute values of the structural responses, the fundamental conclusions of the study remain robust.

Table 13. Sensitivity of the 6-story frame's maximum inter-story drift to damper contribution and steel yield stress.

Design Method	Steel Yield Stress (MPa)	Damping Contribution	Max. Inter-Story Drift (%)
FBD	240	30%	0.76
	240	15%	1.05
	350	30%	0.82
DDBD	240	30%	0.64
	240	15%	0.85
	350	30%	0.68

Reducing the damping capacity, as expected, led to an increase in inter-story drift for both design methods. Similarly, designing with higher-strength steel resulted in more flexible frames and a corresponding slight increase in drift, as member sizes were optimized for strength rather than stiffness. However, across all scenarios, the DDBD-designed frame consistently exhibited a lower maximum drift compared to its FBD-designed counterpart. This confirms that the relative advantages of the DDBD methodology are rooted in its displacement-based design philosophy and are not merely a product of a specific damping level or material grade.

8- Summary and Conclusion

In this investigation, the influence of employing viscous fluid dampers as a passive control mechanism on the structural behavior of three distinct flexural steel frames, comprising three-, six-, and nine-story configurations, was examined. Furthermore, two distinct design methodologies, grounded in force-based and displacement-based principles, were utilized for the structural design. Initially, the two-dimensional frames were designed through equivalent static analyses using the aforementioned methodologies within the SAP2000 software, yielding the corresponding beam and column cross-sections. Subsequently, to assess the efficacy of the viscous dampers, the structures were subjected to nonlinear time history analyses under the influence of seven scaled accelerograms, aligned with the standard design spectrum 2800. The drift and base shear responses of the structures were then systematically compared. The principal findings derived from this study are succinctly summarized as follows:

1. The application of the direct displacement-based design method leads to the adoption of larger cross-sections, consequently resulting in an increased structural weight. Furthermore, the damping coefficients associated with viscous dampers designed through this approach were observed to be significantly higher compared to those derived from the force-based design method.
2. The utilization of a nonlinear viscous damper in both design methodologies has resulted in a reduction of plastic hinges formed within the structure. Furthermore, the magnitude of plastic hinge rotation in structures designed using the force-based method is observed to be greater than that in structures designed employing the displacement-based method.
3. The maximum values derived from the average drift and displacement across various floors of structures incorporating

viscous dampers, with the exception of the nine-story structure designed using force-based criteria, have been observed to exhibit a significant reduction compared to configurations lacking such dampers. Furthermore, dampers designed based on displacement criteria have, in the majority of cases, demonstrated a more pronounced efficacy in mitigating the average displacement and drift within the floors of the structures.

4. The implementation of a viscous nonlinear damper has resulted in a substantial reduction in the average base shear across all structures designed utilizing both force-based and displacement-based methodologies. Notably, the reduction in the average base shear has been observed to be more pronounced in dampers designed according to displacement-based principles. Furthermore, owing to the incremental increase in structural weight associated with the displacement-based design approach, the base shear values derived from this method have been consistently higher compared to those obtained through the force-based design method.

5. In general, it can be concluded that the implementation of nonlinear viscous dampers has effectively mitigated the structural response in the examined cases, ensuring that the responses remain well within the prescribed safety margins relative to code-specified limits. Furthermore, the adoption of the displacement-based direct design method has facilitated the optimal utilization of the structural capacity, enabling the attainment of allowable drift limits associated with the life safety performance level. Additionally, the dampers designed utilizing this methodology have demonstrated exceptional performance, further validating the efficacy of the approach.

6. The distribution of viscous damper coefficients has a substantial impact on seismic performance. The non-uniform distribution resulting from the DDBD method proved to be a more efficient pattern, especially for the 6- and 9-story frames, where it provided significantly better drift control compared to the uniform distribution from the FBD method. This demonstrates that a performance-based design like DDBD not only sizes the dampers correctly but also refines their distribution, which is a critical advantage for taller structures.

7. The initial economic assessment of the sectional data obtained in this study shows that the integration of viscous dampers consistently reduced the required steel cross-sections for both the FBD and DDBD methods, indicating that material savings can offset a portion of the damper cost. The critical trade-off lies in performance versus initial investment. The FBD method with dampers yields the lightest structure but may exhibit less optimal drift control and a less desirable hinge mechanism. Conversely, the DDBD method with dampers provides a superior and more predictable seismic performance, ensuring that the structure meets target displacement objectives reliably. This enhanced performance and potential for reduced damage repairability likely translate to lower life-cycle costs and better loss mitigation, justifying the potential for higher initial damper costs, especially in critical or high-seismicity structures.

8. This study provides specific, data-driven insights to inform the future evolution of seismic design codes. The demonstrated reliability of the DDBD method supports its consideration as an approved alternative procedure, while the superior performance of its non-uniform damper distribution highlights an opportunity to refine force-based design provisions with more efficient guidelines. Furthermore, the successful application of equivalent viscous damping models validates their suitability for codified performance-based approaches. By bridging academic research and practical code development, this work contributes evidence to the broader, ongoing discussion within the engineering community, encouraging further investigation toward more resilient and predictable seismic design.

This study confirms the effectiveness of the DDBD method for low- to mid-rise steel moment frames (up to 9 stories) equipped with viscous dampers. However, it is important to recognize that this work did not cover the behavior of taller structures. The traditional DDBD approach, which relies on a simplified single-degree-of-freedom model, may have limitations in taller frames where higher modes play a more significant role in seismic response. Future research should focus on developing and validating advanced, multi-modal DDBD techniques that use generalized frameworks and substitute structures to accurately assess seismic demands in high-rise buildings.

References

1. Priestley, M. J. N. (2003). Myths and Fallacies in Earthquake Engineering, Revisited: The Ninth Mallet Milne Lecture, 2003. Istituto Universitario di Studi Superiori di Pavia.
2. Priestley, M. N. (1997). Myths and fallacies in earthquake engineering. *Concrete International*, *19*(2), 54-63.
3. Maley, T. J., Sullivan, T. J., & Corte, G. D. (2010). Development of a displacement-based design method for steel dual systems with buckling-restrained braces and moment-resisting frames. *Journal of Earthquake Engineering*, *14*(S1), 106-140.
4. Malla, N., & Wijeyewickrema, A. C. (2021, December). Direct displacement-based design of coupled walls with steel shear link coupling beams. In *Structures* (Vol. 34, pp. 2746-2764). Elsevier.

5. Liu, J., Xu, L., & Xie, X. (2022). Seismic design and performance of a steel frame-shear plate shear wall with self-centering energy dissipation braces structure. *Journal of Building Engineering*, *51*, 104336.
6. Ureña, A. G., Tremblay, R., & Rogers, C. A. (2021). Earthquake-resistant design of steel frames with intentionally eccentric braces. *Journal of Constructional Steel Research*, *178*, 106483.
7. Moradpour, S., & Dehestani, M. (2019, December). Optimal DDBD procedure for designing steel structures with nonlinear fluid viscous dampers. In *Structures* (Vol. 22, pp. 154-174). Elsevier.
8. Alehojjat, S. B., Bahar, O., & Yakhchalian, M. (2021, December). Improvements in the direct displacement-based design procedure for mid-rise steel MRFs equipped with viscous dampers. In *Structures* (Vol. 34, pp. 1636-1650). Elsevier.
9. Mohebbi, M., Noruzvand, M., Dadkhah, H., & Shakeri, K. (2022). Direct displacement-based design approach for isolated structures equipped with supplemental fluid viscous damper. *Journal of Building Engineering*, *45*, 103684.
10. Kalapodis, N. A., Muho, E. V., & Beskos, D. E. (2022). Seismic design of plane steel MRFS, EBFS and BRBFS by improved direct displacement-based design method. *Soil Dynamics and Earthquake Engineering*, *153*, 107111.
11. Shakeri, K., & Dadkhah, H. (2021). Development of DDBD for steel MRFs using inelastic response-based seismic lateral force distribution. *Journal of Building Engineering*, *43*, 103063.
12. Al-Mashaykhi, M., Rajeev, P., Wijesundara, K. K., & Hashemi, M. J. (2019). Displacement profile for displacement based seismic design of concentric braced frames. *Journal of Constructional Steel Research*, *155*, 233-248.
13. Yan, L., & Gong, J. (2019). Development of displacement profiles for direct displacement based seismic design of regular reinforced concrete frame structures. *Engineering Structures*, *190*, 223-237.
14. Seo, C. Y., Karavasilis, T. L., Ricles, J. M., & Sause, R. (2014). Seismic performance and probabilistic collapse resistance assessment of steel moment resisting frames with fluid viscous dampers. *Earthquake engineering & structural dynamics*, *43*(14), 2135-2154.
15. Milanchian, R., & Hosseini, M. (2019). Study of vertical seismic isolation technique with nonlinear viscous dampers for lateral response reduction. *Journal of Building Engineering*, *23*, 144-154.
16. Mirzai, N. M., Attarnejad, R., & Hu, J. W. (2021). Experimental investigation of smart shear dampers with re-centering and friction devices. *Journal of Building Engineering*, *35*, 102018.
17. Luo, Z., Xue, J., Qi, L., & Sui, Y. (2021). Experimental and numerical study on viscously-damped outriggers with amplifying devices. *Journal of Building Engineering*, *38*, 102172.
18. Ramirez, O., Constantinou, M. C., & Kitcher, C. A. (2001). *Development and Evaluation of Simplified Procedures for Passive Energy Disipation Systems*. MCEER-00-0010. Buffalo, NY.
19. ASCE (American Society of Civil Engineers). (2005). Minimum Design Loads for Buildings and Other Structures-ASCE/SEI 7-05. American Society of Civil Engineers.
20. Kitayama, S., & Constantinou, M. C. (2018). Seismic performance of buildings with viscous damping systems designed by the procedures of ASCE/SEI 7-16. *Journal of Structural Engineering*, *144*(6), 04018050.
21. Lin, Y. Y., Tsai, M. H., Hwang, J. S., & Chang, K. C. (2003). Direct displacement-based design for building with passive energy dissipation systems. *Engineering structures*, *25*(1), 25-37.
22. Kim, J., & Choi, H. (2006). Displacement-based design of supplemental dampers for seismic retrofit of a framed structure. *Journal of Structural Engineering*, *132*(6), 873-883.
23. Sullivan, T. J., & Lago, A. (2012). Towards a simplified direct DBD procedure for the seismic design of moment resisting frames with viscous dampers. *Engineering Structures*, *35*, 140-148.
24. Sullivan, T. J. (2009). Direct displacement-based design of a RC wall-steel EBF dual system with added dampers. *Bulletin of the New Zealand Society for Earthquake Engineering*, *42*(3), 167-178.
25. Noruzvand, M., Mohebbi, M., & Shakeri, K. (2020). Modified direct displacement-based design approach for structures equipped with fluid viscous damper. *Structural Control and Health Monitoring*, *27*(1), e2465.
26. Bruschi, E., Quaglini, V., & Calvi, P. M. (2022). A simplified design procedure for seismic upgrade of frame structures equipped with hysteretic dampers. *Engineering Structures*, *251*, 113504.
27. Guo, L., Wang, J., Wang, W., & Wang, H. (2023, November). Performance-based seismic design and vulnerability assessment of concrete frame retrofitted by metallic dampers. In *Structures* (Vol. 57, p. 105073). Elsevier.
28. Li, Z., Cheng, X., Li, Y., & Gao, X. (2024). Substructure-based design method for vertically irregular steel buckling-restrained braced frame structures. *Engineering Structures*, *306*, 117784.

29. Mustafa, Z. N. E., & Saito, T. (2024). Displacement-Based Seismic Design of Multi-Story Resistance Capacitance-Coupled Shear Wall Buildings with Energy-Dissipation Dampers. *Applied Sciences*, *14*(22), 10734.
30. Azizi, H., 2025, July. Numerical evaluation of cyclic and seismic performance of three-core buckling-resistant braces with partially re-centering properties. In Structures (Vol. 77, p. 109078). Elsevier.
31. Azizi, H., & Ahmadi, J. (2024). Investigating the seismic behavior of low-rise steel frames equipped with dual-core self-centering buckling-restrained brace. Soil Dynamics and Earthquake Engineering, 185, 108905.
32. ISIR 2800, Seismic resistant design of buildings (2014) – Code of practice, Standards and Industrial Research of Iran, (in Persian).
33. Iranian code for loading, (2014) "Design loads for building", National Regulation of Building, Part 6, (in Persian).
34. Iranian code for steel structures, (2014) "Design and Construction of Steel Structures", National Regulations of Building, Part 10, (in Persian).
35. Pekelnicky, R., Engineers, S. D., Chris Poland, S. E., & Engineers, N. D. (2012). ASCE 41-13: Seismic evaluation and retrofit rehabilitation of existing buildings. Proceedings of the SEAOC.
36. Ohtori, Y., Christenson, R. E., Spencer Jr, B. F., & Dyke, S. J. (2004). Benchmark control problems for seismically excited nonlinear buildings. Journal of engineering mechanics, 130(4), 366-385.
37. Azizi, H. and Ahmadi, J., 2025. Mitigation of residual deformations in steel braced frames through an innovative Y-shaped hybrid buckling restrained braces. Journal of Constructional Steel Research, 229, p.109533.
38. Azizi, H., & Ahmadi, J. (2024). Seismic Performance Evaluation of Two-and Three-Story Steel Frames with an Upgraded Hybrid Buckling-Restrained Brace. *Iranian Journal of Science and Technology, Transactions of Civil Engineering*, 1-27.
39. Azizi, H., Eghbali, M., & Ahmadi, J. (2024). Numerical Investigation on the Efficiency of Self-Centering Two-Yield Buckling Restrained Brace on Low-Rise Steel Frames. International Journal of Civil Engineering, 1-24.